



Article

Beneficial Microorganisms to Control the Gray Mold of Grapevine: From Screening to Mechanisms

Zakaria Amarouchi ^{1,2}, Qassim Esmaeel ¹, Lisa Sanchez ¹, Cédric Jacquard ¹, Majida Hafidi ²,
Nathalie Vaillant-Gaveau ¹ and Essaid Ait Barka ^{1,*}

- ¹ Université de Reims Champagne-Ardenne, RIBP EA4707 USC INRAE 1488, SFR Condorcet FR CNRS 3417, 51100 Reims, France; zakariaamarouchi@gmail.com (Z.A.); qassim.esmaeel@univ-reims.fr (Q.E.); lisa.sanchez@univ-reims.fr (L.S.); cedric.jacquard@univ-reims.fr (C.J.); nathalie.gaveau@univ-reims.fr (N.V.-G.)
- ² Laboratoire de Biotechnologie Végétale et Valorisation des Bio-Ressources, Faculté des Sciences, Université Moulay Ismail, Meknès B.P. 11201, Morocco; hafidimaj@yahoo.fr
- * Correspondence: ea.barka@univ-reims.fr; Tel.: +33-326913221

Abstract: In many vineyards around the world, *Botrytis cinerea* (*B. cinerea*) causes one of the most serious diseases of aerial grapevine (*Vitis vinifera* L.) organs. The control of the disease relies mainly on the use of chemical products whose use is increasingly challenged. To develop new sustainable methods to better resist *B. cinerea*, beneficial bacteria were isolated from vineyard soil. Once screened based on their antimicrobial effect through an in vivo test, two bacterial strains, S3 and S6, were able to restrict the development of the pathogen and significantly reduced the Botrytis-related necrosis. The photosynthesis analysis showed that the antagonistic strains also prevent grapevines from considerable irreversible PSII photo-inhibition four days after infection with *B. cinerea*. The 16S rRNA gene sequences of S3 exhibited 100% similarity to *Bacillus velezensis*, whereas S6 had 98.5% similarity to *Enterobacter cloacae*. On the other hand, the in silico analysis of the whole genome of isolated strains has revealed the presence of “biocontrol-related” genes supporting their plant growth and biocontrol activities. The study concludes that those bacteria could be potentially useful as a suitable biocontrol agent in harvested grapevine.

Keywords: gray mold; biocontrol; grapevine



Citation: Amarouchi, Z.; Esmaeel, Q.; Sanchez, L.; Jacquard, C.; Hafidi, M.; Vaillant-Gaveau, N.; Ait Barka, E. Beneficial Microorganisms to Control the Gray Mold of Grapevine: From Screening to Mechanisms. *Microorganisms* **2021**, *9*, 1386. <https://doi.org/10.3390/microorganisms9071386>

Academic Editor: Fred O. Asiegbu

Received: 3 June 2021
Accepted: 23 June 2021
Published: 25 June 2021

Publisher's Note: MDPI stays neutral with regard to jurisdictional claims in published maps and institutional affiliations.



Copyright: © 2021 by the authors. Licensee MDPI, Basel, Switzerland. This article is an open access article distributed under the terms and conditions of the Creative Commons Attribution (CC BY) license (<https://creativecommons.org/licenses/by/4.0/>).

1. Introduction

Pathogens cause a devastating impact on crops varying from economic hardship to poisoning of food supplies (such as ergotism) and horrendous famines such as the Irish potato famine that lasted from 1845 to 1852. After their assaults, pathogens might trigger substantial changes to the host physiology, which can occur directly by secreting toxins and lytic enzymes or indirectly through inducing host responses stimulated by the pathogen. Among the significant physiological processes, the photosynthesis is the principal process affected by foliar diseases [1]. The photosynthesis decline might be proportional to decrease in green leafy tissue. Furthermore, the decline in photosynthesis, infections can trigger other physiological changes such as limited water use efficiency, which in turn, excessive water restriction may further induce a lower rate of photosynthesis (as reviewed in [2]). The pathogen might also impact the net carbon assimilation rate by enhancing the leaf respiration, which is requested to supply the demand initiated by the accelerated cells host metabolic activity [3]. The photosynthesis decreases through the infection process as a result of repression of photosynthetic gene expression [4,5]. Despite various struggles to decipher mechanisms by which pathogens can disturb photosynthetic capacity, current knowledges of the subject remain far from inclusive.

Plants do not have a circulatory system and adaptive immune system like animals. To block pathogen progress, plants have evolved a two-layered innate immune system.

The first line of plants defense is accomplished via a set of defined receptors, namely pattern recognition receptors (PRRs), which able to identify conserved microbe-associated molecular patterns (MAMPs) [6]. Following MAMPs recognition, MAMP-triggered immunity (MTI) primary defense responses are triggered including mitogen-activated protein kinase (MAPK) phosphorylation cascades, cell wall alterations, callose deposition, defense genes expression, and defense-related proteins accumulation [7,8].

When perceived by intracellular immune receptors, pathogen effectors trigger the effector-triggered immunity (ETI; [8]). The second stage of perception uses the recognition of microbial effectors, the virulence factors that suppress MTI to initiate effector-triggered immunity (ETI), triggering a cascade of complex signaling events, leading to suppression of pathogen assaults.

Botrytis cinerea is one of the highest broadly studied necrotrophic fungal pathogens. *B. cinerea* has no apparent host specificity infecting therefore, more than 1000 plant species [9]. The gray mold (GM) caused by *B. cinerea* has a devastating impact on various economically important crops, including grape, strawberry, and tomato [10] with annual economic losses exceeding USD 10 to 100 billion worldwide [9,11,12].

Several disease controlling approaches have been implemented in the past and present to control *B. cinerea*. Currently, pesticides remain the main method used to fight the pathogen, and in some instances, the only option, involving significant financial costs. Until lately, the use of chemical fungicides to protect plant was thought to be fairly safe. Nevertheless, more than ever before, chemical fungicides use faces multiple challenges namely the development of resistance to fungicides resulting in the decline or even failure of control effect [13–16], increased consumers desire of food free of pesticide residues [17], enhanced concern regarding environmental pollution, and stricter regulatory policies are being imposed on the use of synthetic chemical fungicides [17,18].

To overcome the difficulties previously stated, it is urgent to search for alternative, effective, and eco-friendly strategy of disease control [19–21]. Thus, in recent years, the use of microbes as a biocontrol agent is gaining interest in agriculture [22].

Plant growth promoting rhizobacteria (PGPR) are bacteria that inhabit the rhizosphere and can improve the extent or quality of plant growth directly and or indirectly. The direct promotion by PGPR involves either delivering plant with a plant growth promoting substances or helping plants to mobilize and acquire nutrients from the rhizosphere. The indirect effect occurs when PGPR prevent the harmful effect of pathogens. In the last few decades, bacteria including species of *Arthobacter*, *Azospirillum*, *Azotobacter*, *Bacillus*, *Burkholderia*, *Enterobacter*, *Klebsiella*, *Pseudomonas*, and *Serratia* have reported to enhance plant fitness.

Various mechanisms for antagonism have been implicated, such as competition for nutrients and space, secretion of cell wall degrading enzymes, siderophores [23,24], parasitism of the pathogen, biofilm formation, induction of host defenses via production of various pathogenesis related proteins (PR) [25], and the involvement of reactive oxygen species (ROS) in the defense response are responsible for their antagonistic activity [18]. PR proteins regulated resistance in response to *B. cinerea* in grapes. Therefore, nitrogen and carbon metabolisms play critical roles in the resistance of grapes against *B. cinerea* [26]. However, the main inhibitory action of antagonistic bacteria is to produce antifungal metabolites and antibiotics [27,28].

Given the wide-ranging and the importance of *B. cinerea* in agriculture, the control of GM is of great concern. In this context, our strategy was to develop new biotechnologies allowing grapevine to better resist parasitic pressures of *B. cinerea* through the isolation and screening of beneficial bacteria. Once screened, the mechanisms contributing to the biocontrol effect of selected bacteria was deciphered by determining their antimicrobial effect by in vivo test, and finally chlorophyll fluorescence imaging after *Botrytis* challenge. On the other hand, the in silico analysis of the whole genome of isolated strains has revealed the presence of “biocontrol-related” genes supporting their plant growth and biocontrol activities.

2. Materials and Methods

2.1. Soil Sampling

Soil samples were collected from different distinct locations of vineyard (Chardonnay cv.) in Meknes-Morocco. Sampling was carried out at the end of the growing season, after the occurrence of the asexual multiplication of *B. cinerea* and the appearance of symptoms of gray rot detectable on the grapevine. Although isolation of antagonistic bacterial strains was taken from soil samples of healthy grapevine, the bacteria coming from soil collected under the infected plants were selected as control, to compare the communities of both populations. At each sampling points, soil was collected aseptically from healthy and severely infected grapevines with *B. cinerea*. Samples were kept in paper bags placed in ice and processed within 24 h.

2.2. Isolation, Purification, and Enrichment of Antagonistic Bacteria

The isolation of bacteria was carried out according to the protocol previously described by Nally et al. [29], with some modifications. Portions of 15 g of Rhizospheric soils were suspended in 250 mL of sterile Luria-Bertani (LB) liquid medium (tryptone 10 g/L; yeast extract 5 g/L; NaCl 10 g/L; pH 7.2). The enrichment culture was incubated on a rotary shaker (180 rpm) at 28 °C for 24 h. This operation was repeated for the soil recovered under the vines showing the GM symptoms. After shaking, the cultures were kept undisturbed for 30 min. Then, isolation of viable bacterial cultures from soil suspensions was done by serial dilution plate count in phosphate-buffer saline (PBS 10 mM, pH 6.5). Aliquots of 100 µL from the five different dilutions of the sequential enrichment were spread in triplicate on LB medium and incubated at 28 °C for 24–72 h until colony development. Colonies with distinct morphologies were picked and purified using the streaking method. The purified isolates were used to screen antagonistic bacteria against *B. cinerea*. Afterwards, pure bacterial cultures were maintained in cryovials containing LB broth with 25% glycerol and preserved at –80 °C.

2.3. In Vitro Screening of Potential Antagonistic Bacteria

Isolated strains were tested for antifungal activity against *B. cinerea*. Assays were performed by patching, in the middle of PDA medium (Sigma-Aldrich, MO, USA) plates, 5 mm of agar plug carrying freshly grown culture of the fungal pathogen. After that, a volume of 5 µL of suspension of each isolate was drooped at four sites approximately 1 cm from the rim of the plate and incubated at 22 °C for five days at which point we start measurements. Plates inoculated with *B. cinerea* were also used as control. The plates were visually inspected for the presence of inhibition zones between the fungus and the colonies considered to be potential antagonistic bacteria. The antifungal effect was estimated by calculating the percentage of inhibition (%) of mycelial growth measured as follows:

$$I(\%) = (1 - C_n / C_o) \times 100 \quad (1)$$

where “C_n” is the average diameter of the mycelial in the presence of the antagonists and “C_o” the average diameter of the control. Experiments were conducted in duplicate and the results reported are averages of three independent experiments. The diameter of the clear zones depends on the performance of the bacteria. Thus, the screened strains with high zones of clearing were selected for molecular identification and in vivo assays.

2.4. Identification of Antagonistic Bacteria

All potential antagonistic bacteria were identified by 16S rRNA gene analysis. The 16S rRNA gene was amplified by polymerase chain reaction (PCR) as previously described by [30]. Briefly, genomic DNA was extracted from a pure colony using the Wizard Genomic Purification DNA Kit (Promega Corp., Madison, WI, USA), according to the manufacturer’s instructions. Next, the bacterial 16S rRNA gene was amplified by PCR using FD2 (5- AGAGTTTGATCATGGCTCAG -3) and RP1(5- ACGGTTACCTTGTTACGACTT -3)

primers. The PCR was carried out with a 50- μ L final volume, containing 25- μ L of Master Mix (Thermo Scientific Fermentas, Villebon sur Yvette, France), 2.5 μ L of each primer, 15 μ L sterile water, and 5 μ L template DNA in a PTC-200 Thermocycler (C1000 touch thermal cycler, Bio-Rad, Hercules, CA, USA). The PCR conditions used were as follows: an initial denaturation step at 94 °C for 5 min, followed by 30 cycles of denaturation at 94 °C for 45 s, primer annealing at 55 °C for 45 s, and elongation at 72 °C for 1.5 min, and a final elongation step at 72 °C for 10 min.

The PCR product was subjected to electrophoresis on agarose gel with 0.5X TAE buffer (Tris Acetate-EDTA) at a ratio of 1% (weight/volume). Gels were stained with ethidium bromide, visualized under UV light (300 nm), and were then excised and purified using the GeneJET Gel Extraction Kit (Thermo Scientific Fermentas, Waltham, USA), as recommended by the manufacturer. A 1000-bp DNA ladder marker served as the standard size. The PCR product was commercially sequenced by Genewiz Co., Ltd. (Leipzig, Germany). The data output was analyzed, and the sequences were compared with sequences in the National Center for Biotechnology Information (NCBI) database using the BLAST search program (<http://www.ncbi.nlm.nih.gov/>). Alignment of *16S rRNA gene* sequences from GenBank database was performed using ClustalX 1.8.3 with default settings [31]. Phylogenesis was analyzed by MEGA version 7. Distances were calculated using the Kimura two parameter distance model. The tree was built by the neighbor-joining method. The dataset was boot- strapped 1000 times [32].

2.5. Biochemical Characterization of Biocontrol Isolates

Biochemical characteristics of isolated strains such as carbohydrate assimilation and fermentation were performed using BIOLOG GENIII microtiter plate (Hayward, CA, USA) as recommended by manufacturers.

2.6. Cellular Fatty Acid Analysis

Cellular fatty acid analysis was carried out at BCCM/LMG (the Belgian Co-ordinated Collections of Microorganisms, Ghent University, Ghent, Belgium). Bacterial isolates were grown for 24 h at 30 °C under aerobic conditions on LB medium. Inoculation and harvesting of the cells, and the extraction and analysis were performed conform to the recommendations of the commercial identification system MIDI (Microbial Identification System, Inc., Newark, DE, USA). The whole-cell fatty acid composition was determined gas chromatographically on an Agilent Technologies 6890N gas chromatograph (Santa Clara, CA, USA). The peak naming table MIDI TSBA 5.0 was used.

2.7. Whole Genome Sequencing, Assembly, and Annotation

The genomic DNA of strains was isolated using the Wizard Genomic Purification DNA Kit (Promega Corp., Madison, WI, USA) according to the manufacturer's instructions. The integrity of extracted DNA was assessed by running the sample on 1% agarose gel. The genome sequence of the strain was sequenced at MicrobesNG (<http://www.microbesng.uk>) using the method summarized in Table S1. The draft genome sequences were used for annotation using the Rapid Annotation Subsystem Technology (RAST) server (<http://rast.nmpdr.org>) [33]. The annotated genes were analyzed using SEED database [34]. To predict the presence of secondary metabolites (SMs) gene clusters associated with biocontrol activity, the draft genome sequence was analyzed by antiSMASH software online (<https://antismash.secondarymetabolites.org/#!/start>) [35]. The Whole Genome Shotgun projects of the strains have been deposited in GenBank under the accession numbers JAFETM000000000 and JAFETL000000000. The version described in this paper version JAFETM010000000 and JAFETL010000000, respectively.

2.8. Grapevine In Vitro Plantlets

Plantlets of *Vitis vinifera* cv. Chardonnay (clone 7535) were micro-propagated by nodal explants grown on 15 mL of Murashige-Skoog (MS) agar medium in 25 mm-culture

tubes as described by Ait Barka et al. [36]. Cultures were performed in a growth chamber under white fluorescent light ($200 \mu\text{mol}/\text{m}^2/\text{s}$), with 16 h/8 h day/night photoperiod at a constant temperature of 26°C .

2.9. Bacterial Isolates and Inoculum Preparation

Bacterial suspensions were prepared by inoculating 100 mL of Luria-Bertani (LB) liquid culture medium and incubated on a rotary shaker at 180 rpm at 28°C for 18 h at which point they reached the late exponential growth phase. After incubation, cells were harvested by centrifugation at $4500 \times g$ at 4°C for 15 min. Each culture was washed three times and resuspended in 20 mL of phosphate-buffered saline (PBS). The density of bacterial cultures was determined by spectrophotometry and adjusted at approximately 10^8 colony-forming units (CFU) mL^{-1} with an optical density 0.8 at 600 nm (OD_{600}).

For the inoculum preparation, the fungal pathogen, *B. cinerea* strain 630 was grown on potato dextrose agar (PDA) (Sigma-Aldrich, MO, USA) at 22°C . The conidia were collected from 20-day-old culture plates by scratching the Petri dishes surface with sterile potato dextrose broth (PDB 24 g/L) medium and filtered to remove hyphae. Conidial concentrations were measured by a hemocytometer and the final density was adjusted to 10^5 conidia/mL. After incubation during 3 h at 22°C and 150 rpm, the resulting germinated spore suspension was used for plant inoculation.

2.10. Inoculation of In Vitro Plantlets with Antagonistic Bacteria and Infection by *B. cinerea*

Isolates with higher percentage of inhibition (%) during in vitro screening were tested for antagonistic activity against *B. cinerea* on sterile grapevine plantlets. Briefly, roots of 6-weeks-old grapevine plantlets were gently removed from the MS agar medium (Sigma-Aldrich, France) and transferred into magenta boxes containing 120 g of soil. Plantlets were then inoculated with bacterial inoculum at a concentration of 10^8 CFU per g of soil. Control was treated with sterile PBS. Bacterized and non-bacterized plantlets were then grown for an additional 10 days. Thereafter, the upper side of each leaf was inoculated by a drop of $5 \mu\text{L}$ of *B. cinerea* germinated spore suspension. This protocol was used for measures of necrosis surfaces. The antifungal effect was estimated by calculating the percentage of inhibition (%) of mycelial growth measured as describes in in vitro tests.

For IMAGING-PAM analysis, plantlets were sprayed with the germinated spore suspension of *B. cinerea* to have a homogenous application. Plantlets were then placed in growth chamber at 22°C . All the experiments were performed in triplicate.

2.11. IMAGING-PAM Analysis

Chlorophyll fluorescence parameters were measured with an IMAGING-PAM measuring system (Heinz Walz, Germany) using the saturation pulse method [37]. Control and bacterized plantlets were dark adapted for 30 min to establish the minimal fluorescence level (F_0) and the maximal fluorescence (F_m) after a saturating flash (1 s ; $13,000 \mu\text{mol}/\text{m}^2/\text{s}$). Each leaf was detached from the plantlet then exposed immediately to an actinic illumination of $79 \mu\text{mol}/\text{m}^2/\text{s}$. After fluorescence stabilization, a second saturating flash was imposed to determine the maximal fluorescence (F_m') of light-adapted inflorescences. The effective PSII quantum yield, ΦPSII , is calculated according to the equation of Genty et al. [38]. The quantum yield of regulated energy dissipation in PSII, ΦNPQ , and the quantum yield of nonregulated energy dissipation in PSII, ΦNO , was calculated according to Kramer et al. (2004) [39]. Please note that $\Phi\text{PSII} + \Phi\text{NPQ} + \Phi\text{NO} = 1$. The data were collected taking in consideration the entire leaf area including necrosis area. Measurements were taken 24 h before inoculation of antagonistic bacteria, 24 h before infection with *B. cinerea*, and 4 consecutive days after infection. The means \pm standard deviations originated from three independent experiments realized in duplicates, each replicate consisted of four plantlets.

2.12. Statistical Analysis

The experimental design used was performed in triplicates. Statistical analyses were carried out using GraphPad Prism version 5.00 for Windows (GraphPad Software, San Diego, CA, USA) (www.graphpad.com). For lesion diameter Student's *t*-tests ($\alpha > 0.05$) was used to compare lesion area between inoculated and non-inoculated plants.

3. Results

3.1. Isolation and In Vitro Screening of Antagonistic Bacteria

As a result of multiple inoculations and purification, 42 pure cultures of potential antagonistic bacteria were successfully enriched and isolated from vineyard soil. These freshly isolated strains were purified on LB plates, selected based on their morphology, and used as objects of investigation. All isolates were screened for their ability to inhibit the mycelial growth of *B. cinerea* by direct confrontation tests in PDA medium plates. Out of 42 tested strains, only two isolates were estimated as antagonistic potential bacteria against this fungus. They were nominated S3 and S6 which were the most active against fungal culture, by showing the strong percentage of inhibition I (%) (Figure 1A). These isolates were tested for their ability to protect grapevines against GM *in planta*.

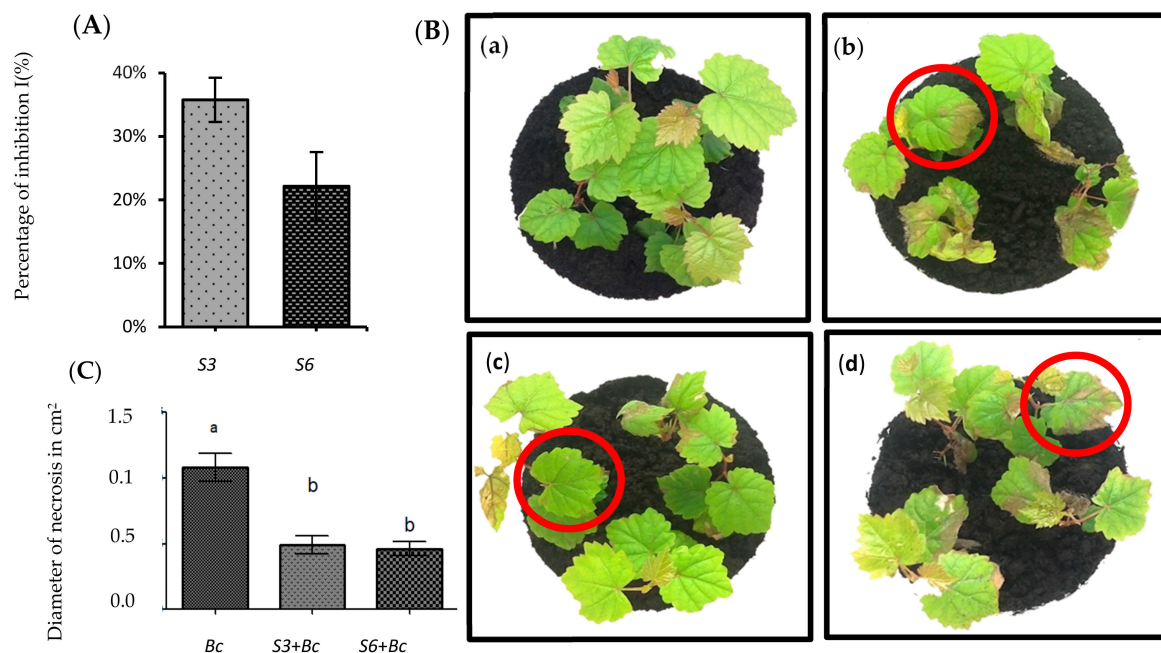


Figure 1. Impact of isolates on *B. cinerea* growth inhibition. Direct confrontation tests of isolates against *B. cinerea*. Results indicated are the mean of percent inhibition of mycelial growth of *B. cinerea* after 72 h of incubation in PDA medium (A). The Ability of isolate to protect grapevines (cv. Chardonnay), in planta, against *B. cinerea* (B,C). In vitro grapevine plantlets inoculated or not with S3 and S6, 72 hours post infection (hpi) with *B. cinerea* (B). (Control, (a); *B. cinerea*, (b); S3 + Bc, (c); S6 + Bc, (d)). Diameter of necrosis measured on leaves infected with *B. cinerea* (C).

3.2. Disease Symptoms Were Significantly Reduced in Root-Bacterized Plantlets

To test the ability of S3 and S6 to protect grapevine in our system, we performed infection on whole potted-plant with *B. cinerea* strain 630 in control versus root-bacterized plantlets. Assays performed showed that the two antagonistic bacteria had high inhibiting ability against *B. cinerea* in grapevines three days after inoculation of the pathogen. They significantly reduced Botrytis-related necrosis by approximately 50% at 72 hpi (Figure 1B). In addition, disease symptoms were significantly less developed in bacterized plants, confirming the protective impact of S3 and S6 against *B. cinerea* (Figure 1C). Non-bacterized plantlets showed severe symptoms typical of GM, manifesting as necrosis around the infection spot (Figure 1C). In contrast, plants treated with the antagonistic bacteria exhibited a

reduction in disease symptoms, displayed by a smaller size of necrosis diameter compared to the control. These isolates were selected for molecular investigation.

3.3. Identification of Antagonistic Bacteria

The molecular identification using *16S rRNA* gene sequences of the antagonistic rhizobacteria show that *S3* and *S6* are closely related to *Bacillus velezensis* (100%), and *Enterobacter cloacae* (98.5%), respectively (Figure 2). Strains *S3* and *S6* also shared sequence identity with other species including *B. subtilis* (99%), and *Pantoea agglomerans* (98%), respectively (Figure 2). Both bacterial strains (*S3* and *S6*) isolated under healthy canopy, were used for further characterization. In addition, to calculate the pair-wise average nucleotide identity (ANI) values of both strains with their closest known relatives, the draft genome sequences of strains *S3* and *S6* were compared against all type strain genomes available in the microbial genomes atlas (MiGA) webserver [40]. Results showed that strains *S3* belongs to *Bacillus velezensis* (99% ANI). For strain *S6*, the closest relatives found was *Enterobacter cloacae* (98% ANI). Moreover, digital DDH values of both strains were compared against all type strain genomes available in the TYGS database [41]. The analysis generated DDH values more than 70% for both strains and the closest relatives were *Bacillus velezensis* and *Enterobacter cloacae* for strains *S3* and *S6*, respectively.

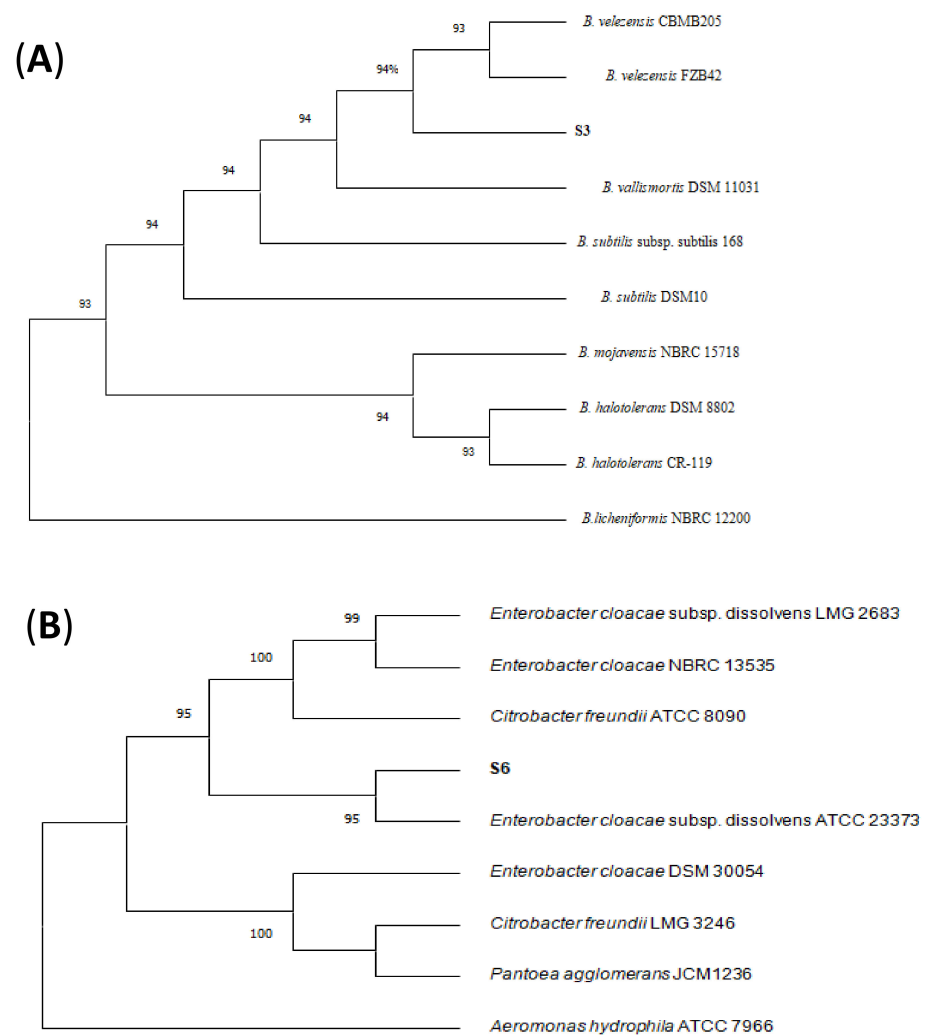


Figure 2. Neighbor-joining phylogenetic tree based on the 16S rRNA sequences of antagonistic isolates *S3* and *S6*, showing the relationship with the genus *Bacillus* (A) and *Enterobacter* (B). The sequence of *B. licheniformis* NBRC 12200 and *Aeromonas hydrophila* ATCC 7966 were chosen as an out-group. Antagonistic strains are shown in bold.

3.4. Characterization of Biocontrol Isolates

The data presented in Table 1 showed some biochemical characteristics of isolated strains. The selected antagonistic isolates (S3 and S6) were characterized by biochemical methods. The optimum growth conditions of isolates are at 28°C, pH 6.0, and in the presence of 1% NaCl. Although cells of strain S3 were sensitive to fusidic acid, minocycline, naldixic acid, rifamycin SV, Incomycin, and vancomycin, strain S6 was resistant to them. Isolates were able to grow in the presence of sodium butyrate, guanidine HCl, lithium chloride, potassium tellurite, and tetrazolium violet, but did not grow in the presence of sodium bromate, D-serine, and niaproof 4 except *E. cloacae*, which was resistant (Table 1). The two isolates failed to hydrolyze gelatin. Furthermore, the strains showed different abilities to use different carbon sources (Table 1). They were able to assimilate, D-cellobiose, mannose, mannitol, and N-acetyl-glucosamine, L-glutamic acid, sucrose, L-aspartic acid, D-maltose, D-fucose (except *B. velezensis* S3), and L-histidine, as sole carbon sources whereas, 3-methylglucose, α -ketobutyric acid, and D-aspartic acid were not used by both strains. The isolates exhibited different patterns of cellular fatty acids profile features characterized by different level of C15: 0 iso-anteiso, C17: 0 iso-anteiso, summed feature 2 (comprising C12: 0 aldehyde, C14: 0 3-OH/ C16: 1 iso I and/or unknown ECL 10.928), C18:1 ω 7c, C16: 0, C17:0 cyclo, C14:0, summed feature 3 (comprising C16:1 ω 7c/15 iso 2OH), C12: 0, and C19: 0 cyclo ω 8c. *Isolate S3* was characterized by a fatty acid profile dominated to an unusual extent (> 98%) by saturated fatty acids (Figure S1). Hence, cells had less iso odd-numbered fatty acid and more anteiso odd-numbered fatty acid, with the major fatty acid being anteiso-C15:0(37.18%) (Table 1). Cells of strain S6 exhibited only 37,88% of saturated fatty acids but revealed other structure as branched chain (29,51%), cyclopropane (16,90%), and hydroxy unsaturated (14.68%) fatty acids that was deficient in strain S3 (Figure S2). The major fatty acid for S6 were C16:0 (18.07%) (Table 2).

Table 1. Biochemical characteristics for the antagonistic strains based on BIOLOG GENIII microtiter plate (Hayward, CA, USA).

| | Oxidation of | | | Oxidation of | | | Oxidation of | |
|----------------------------------|--------------|-----------|----------------------------------|--------------|-----------|----------------------------------|--------------|-----------|
| | S6 | S3 | | S6 | S3 | | S6 | S3 |
| 3-methylglucose | – | – | D-melibiose | + | + | L-lacticacid | + | + |
| Aceticacid | + | – | D-raffinose | + | – | L-malicacid | + | + |
| acetoaceticacid | – | – | D-saccharicacid | + | ± | L-pyroglutamicacid | ± | ± |
| bromo-succinicacid | + | – | D-salicin | ± | – | L-rhamnose | + | – |
| Citricacid | + | ± | D-serine | – | – | L-serine | + | – |
| D-arabitol | ± | – | D-sorbitol | + | + | Methylpyruvate | + | ± |
| D-asparticacid | – | – | D-trehalose | + | + | mucicacid | + | ± |
| D-cellobiose | + | + | D-turanose | ± | ± | myo-inositol | + | ± |
| Dextrin | ± | + | Formicacid | ± | – | N-acetylneuraminicacid | – | ± |
| D-fructose | + | + | Gelatin | – | – | N-acetyl-D-galactosamine | + | ± |
| D-fructose-6-PO4 | + | ± | Gentiobiose | + | – | N-acetyl-D-glucosamine | + | + |
| D-fucose | ± | – | Glucuronamide | + | + | N-acetyl- β -D-mannosamine | + | + |
| D-galactose | + | – | Glycerol | + | ± | Pectin | ± | ± |
| D-galacturonicacid | + | + | Glycyl-L-proline | + | – | p-hydroxyphenylaceticacid | ± | – |
| D-gluconicacid | + | + | Inosine | + | ± | propionicacid | – | – |
| D-glucose-6-PO4 | + | ± | L-alanine | + | + | Quinicacid | – | ± |
| D-gluconicacid | + | + | L-arginine | ± | + | Stachyose | + | – |
| D-lacticacidmethylester | ± | ± | L-asparticacid | + | + | Sucrose | + | + |
| D-malicacid | – | – | L-fucose | ± | – | Tween 40 | – | ± |
| D-maltose | + | + | L-galactonicacid lactone | + | + | A-D-glucose | + | + |
| D-mannitol | + | + | L-glutamicacid | + | + | | | |
| D-mannose | + | + | L-histidine | + | + | | | |
| Growth in the presence of | S6 | S3 | Growth in the presence of | S6 | S3 | Growth in the presence of | S6 | S3 |
| 1% Nacl | + | + | Lincomycin | + | – | Rifamycin SV | + | – |
| 4% Nacl | + | + | Lithiumchloride | + | + | Sodium bromate | – | – |
| 8% Nacl | ± | ± | Minocycline | ± | – | Sodium butyrate | + | + |
| 1% sodium lactate | + | + | Nalidixicacid | ± | – | Tetrazoliumblue | + | – |
| Aztreonam | ± | – | Niaproof 4 | + | – | Tetrazolium violet | + | ± |
| D-serine | – | – | pH 5 | ± | – | Troleandomycin | + | – |
| Fusidicacid | ± | – | pH 6 | + | + | Vancomycin | + | – |
| Guanidinehcl | + | + | Potassium tellurite | + | + | | | |

Table 2. Major cellular fatty acid content of S3 and S6 strains.

| Structure | Fatty Acid | Systematic Name Saturated | % In Isolated Strains | |
|---------------------|-------------------|---|-----------------------|-------|
| | | | S3 | S6 |
| Saturated | C12: 0 | Dodecanoic | 4.23 | 7.52 |
| | C13: 0 | Tridecanoic | - | 1.68 |
| | C13: 0 ANTEISO | | 0.40 | - |
| | C14: 0 | Tetradecanoic | 1.01 | 8.23 |
| | C14: 0 ISO | | 1.11 | - |
| | C15: 0 ISO | | 11.95 | - |
| | C15: 0 ANTEISO | | 37.18 | - |
| | C16: 0 | Hexadecanoic | 17.16 | 18.07 |
| | C16: 0 ISO | | 2.41 | - |
| | C17: 0 | Heptadecanoic | 0.57 | 2.38 |
| | C17: 0 ISO | | 9.44 | - |
| | C17: 0 ANTEISO | | 11.64 | - |
| | C18: 0 | Octadecenoic | 1.21 | - |
| Hydroxy Unsaturated | C15: 0 3-OH | 3- Hydroxy- pentadecenoic | - | 0.58 |
| | C16: 1 ω 5c | cis-11-Hexadecenoic | - | - |
| | C16: 1 ω 11c | | 1.69 | - |
| | C17:1 ω 8c | | - | 0.60 |
| | C18: 1 ω 7c | cis-11- Octadecenoic | - | 13.49 |
| Cyclopropane | C17: 0 cyclo | Cyclo-heptadecanoic | - | 15.04 |
| | C19: 0 cyclo ω 8c | 9-(2-ethylcyclopropyl) Nonanoic | - | 1.86 |
| Branched chain | Summed feature 1 | C 15:1 ISO H/ C 13:0 3OH C 15:1 ISO I/ C 13:0 3OH | - | 3.28 |
| | Summed feature 2 | C12: 0 aldehyde, C 16:1 ISO I/ C 14:0 3OH and/or unknown ECL 10.928 | - | 17.85 |
| | Summed feature 3 | C 16:1 ω7c/ 15 iso 2OH | - | 8.38 |

3.5. Genomic Feature and In Silico Analysis

As summarized in Table 3, the draft genome sequence of the strain S3, assembled into 21 contigs, consists of 4157, 680p with a 46.35% G+C. Strain S6, grouped into 30 contigs exhibited genome size of 4, 604, 658bp, and the GC content was 55.90%. The total number of predicted protein-coding sequences and RNAs was 4316 and 98 of RNAs for S3 versus 4228 and 116 of RNAs in S6, respectively. The genome characteristics of each isolate were detailed in Table 3. The predicted coding sequences (CDS) of S6 were classified into 560 subsystems, most of which were involved in amino acids and derivatives synthesis, carbohydrate and protein metabolism, cofactors, vitamins, prosthetic groups and pigment formations, and stress response (Figure S2). Based on phylogenetic analysis, chemical characteristics, and genotypic data described in this report, the isolate S3 belongs to *B. velezensis* while S6 is attributed to *E. cloacae* species. The draft genome sequence of each isolate was subject to multiple genomic analyses with the aim to identify all the genes potentially responsible for its antimicrobial activity especially those produced by non-ribosomal peptides synthetases (NRPSs). The in silico analysis using antiSMASH server revealed the presence of different secondary metabolites gene clusters (SMGCs) involved in biocontrol. The draft genome of S3 predicted the presence of many SMGCs, including bacillibactin, fengycin, surfactin and bacillaene. In our analysis of S6 genome, we detected the presence of non-ribosomal peptide (NRPs) and bacteriocin.

Table 3. Genomic feature and in silico analysis of draft genome sequences of bacterial isolates.

| Attribute | S3 | S6 |
|-------------------------|----------------------|-------------------|
| Size (bp) | 4.15 Mb | 4.60 Mb |
| G+C content (%) | 46.35 | 55.90 |
| RNA genes | 98 | 101 |
| Protein-coding genes | 3983 | 4258 |
| N50 | 959,830 | 319,447 |
| L50 | 2 | 4 |
| Number of Subsystems | 328 | 560 |
| Most frequently species | <i>B. velezensis</i> | <i>E. cloacae</i> |
| Number of contigs | 21 | 30 |

3.6. Antagonistic Strains Prevent Plants from Considerable Photo-Inhibition of PSII after Pathogen Challenge

To evaluate the effect of root inoculation with *B. velezensis* S3 and *E. cloacae* S6 on photosynthesis before and 24, 48, 72, and 96 h post-infection with *B. cinerea*, changes in excitation flux at PSII were monitored. Photosynthetic parameters including effective PSII quantum yield $Y(II)$, quantum yield of nonregulated energy dissipation $Y(NO)$, quantum yield of regulated energy dissipation $Y(NPQ)$, and maximum PSII quantum yield (F_v/F_m) were evaluated. The false-color scales shown at the bottom of the fluorescence images indicate the amplitude of the particular parameter (Figure 3a). Before infection with the pathogen, no significant difference between bacterized and non-bacterized plantlets was observed regarding the monitored photosynthetic parameters. The value F_v/F_m were around 0.8 before the infection (Figure 3b). Furthermore, no significant fluctuation was occurred in F_v/F_m value in plantlets during 3 days after infection. However, considerable PSII photo-inhibition was observed when plants were not treated with bacteria and were exposed to a prolonged infection with *B. cinerea* (Figure 3b), while at the same time, in response to *B. cinerea*, bacterized plantlets exhibit indistinct symptoms (Figure 3a), and F_v/F_m value remain constant during kinetics (Figure 3b). Best results were displayed by the two strains. In the case of bacterized plantlets, the higher effective quantum yield of photochemical energy conversion in PSII $Y(II)$ was maintained before as well at 96 hpi with *B. cinerea* in comparison to the non-bacterized plant, which decreased. The quantum yield of regulated energy in PSII $Y(NPQ)$ was down-regulated before infection, compared to control. In contrast, four days after infection, the bacterized plantlets dissipated a higher $Y(NPQ)$ than control (Figure 3c). Although no difference in the quantum yield of nonregulated energy loss in PSII $Y(NO)$ was observed between plantlets before infection, this response resulted in a lower $Y(NO)$ in bacterized plantlets after a prolonged infection with *B. cinerea*.

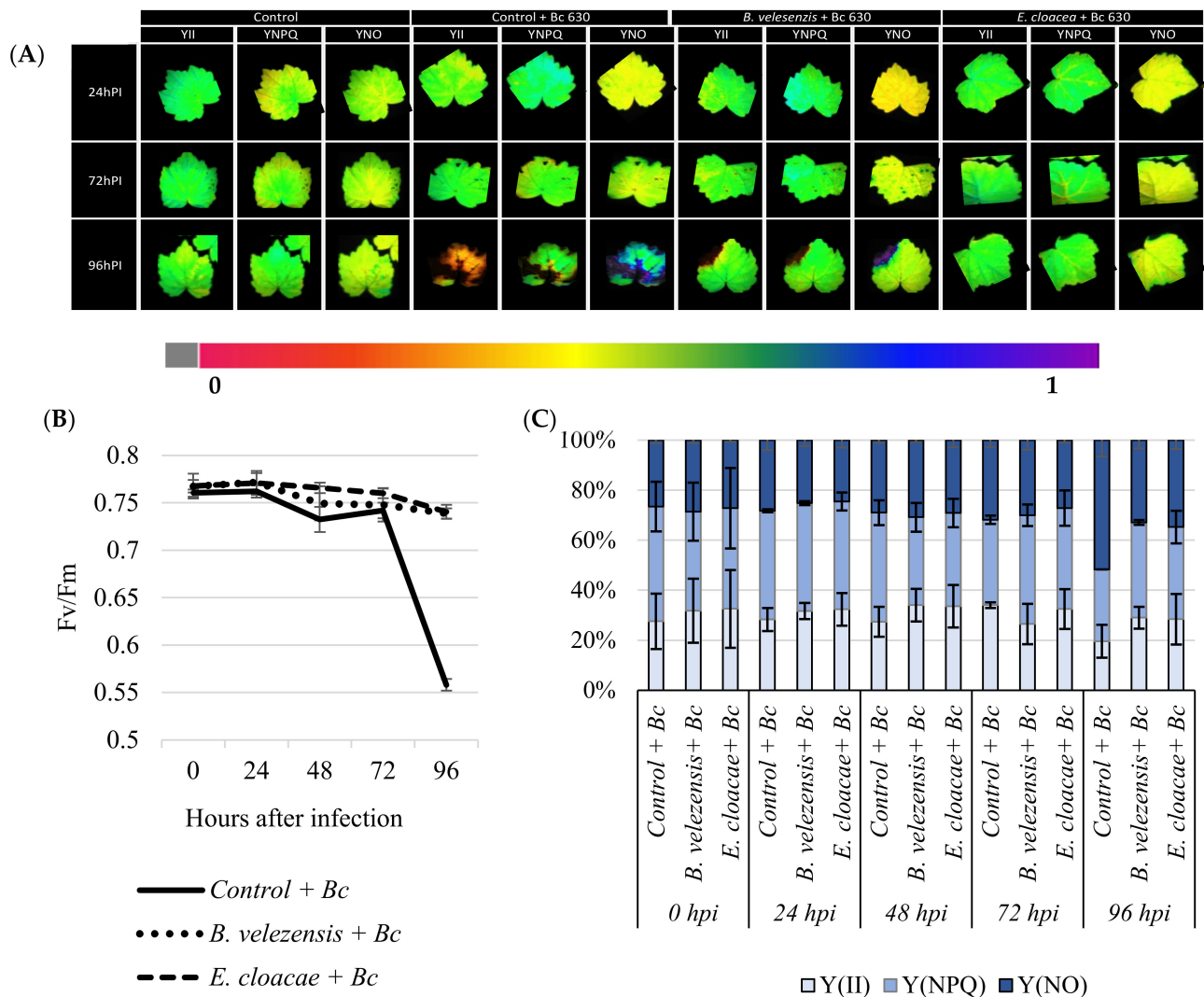


Figure 3. *B. velezensis* S3 and *E. cloacae* S6 prevent grapevines from PSII photo-inhibition four days after infection with *B. cinerea*. Images of the effective PSII quantum yield Y(II), the quantum yield of regulated energy dissipation Y(NPQ) and of nonregulated energy dissipation Y(NO), from grapevine leaves inoculated or not with *B. velezensis* S3 and *E. cloacae* S6 0, 24, 48, 72, and 96 hpi with *B. cinerea*. The pixel value display is based on a false-color scale ranging from black (0.000) via red, yellow, green, blue, to purple (ending at 1.00). The figure shows representative images of one from two independent experiments (A). Evolution of the maximum PSII quantum yield (Fv/Fm) from grapevine leaves inoculated or not with *B. velezensis* S3 and *E. cloacae* S6 0, 24, 48, 72, and 96 hpi with *B. cinerea* (B). Changes in chlorophyll fluorescence parameters (Y(II), Y(NO), and Y(NPQ)) from grapevine leaves inoculated or not with *B. velezensis* S3 and *E. cloacae* S6 0, 24, 48, 72, and 96 hpi with *B. cinerea*. Excitation flux at PSII in infected leaves (C). Values shown are means \pm SD of two independent repetitions (each repetition was realized in triplicates).

4. Discussion

Rhizosphere is an extremely competitive environment, where diverse genera of microorganisms are constantly competing for resources and with each other to survive [42]. This work was undertaken to screen efficient competitive strains from vineyard to control grapevine GM. Among 42, two strains (S3 and S6) have been showed the best performance against the *B. cinerea*. When plantlets were previously bacterized with S3 or S6 then infected with the *B. cinerea*, the symptoms of gray mold were reduced compared to control, confirming therefore the beneficial effect of these strains as reported in in vitro confrontation test. Similar results were reported by Miotto-Vilanova et al., [37] when grapevine plantlets were previously bacterized with *Burkholderia phytofirmans* PsJN before infection with *B. cinerea*.

The 16S rRNA gene sequences of S3 exhibited 100% similarity to *B. velezensis*, while the strain S6 showed 98.5% similarity to *E. cloacae*. *B. velezensis* and *E. cloacae* have been frequently reported as plant growth promoting bacteria and/or biocontrol agents [43–50]. The fact that many *Bacillus* species have very close phenotypic and physiological properties as well as 16S rRNAs gene sequences makes their classification very difficult [51]. The *Bacillus* genus encompasses a large genetic biodiversity [52], and in addition to the “original members” *B. subtilis*, *B. licheniformis* and *B. pumilus*, earlier described by Gordon et al. [53], many novel species belonging to the *B. subtilis* species complex have been described in recent decades, among them *B. amyloliquefaciens* [54], *B. velezensis* [55], and *B. methylotrophicus* [56]. Recently, these *Bacillus* species have been reclassified by genome comparisons and phylogenomic analyses [57]. In particular, *B. methylotrophicus* and *B. amyloliquefaciens* subsp. *plantarum* were later confirmed as heterotypic synonyms of *B. velezensis* [58]. Hence, many studies have suggested that *B. amyloliquefaciens* subsp. *Plantarum*, *B. methylotrophicus*, and *B. velezensis* formed a monophyletic group [59,60].

The plant growth-promoting ability has been related to distinctive physiological activities and molecular changes that might have an intense impact on the fitness (growth and/or health) of plants. Both *B. velezensis* S3 and *E. cloacae* S6 have triggered the resistance of grapevine toward GM disease. *B. velezensis* is a heterotypic synonym of *B. methylotrophicus*, *B. amyloliquefaciens* subsp. *plantarum*, and *B. oryzicola*, and is used to control plant fungal diseases [61] such as *B. cinerea* [62–64]. *Bacillus* species are promising agent for the biological control of postharvest diseases [52], particularly *B. velezensis*, which is widely used in agriculture [65]. Additionally, Morales-Cedeño et al. [66] showed that *B. velezensis* BLE7 showed similar activities to thiabendazole, a commonly used fungicide for *B. cinerea* [67]. In cells of *B. velezensis*, the composition of iso and anteiso fatty acids was higher. The a-C15:0 became even more prominent component of the fatty acids. Furthermore, the major changes observed were a sharp decrease in a-C17:0 content in parallel with a significant increase in a-C15:0. The shift to a fatty acid profile dominated by a-C15:0 draws attention to the critical role of this fatty acid in low temperatures (4 °C) growth [68], presumably due to its physical properties and their effects in maintaining a fluid, liquid-crystalline state of membrane lipids [69], making this bacterium a potential effective biocontrol agent in extreme environments.

Enterobacter cloacae is perhaps best known as an opportunistic human pathogen that is commonly found in hospitals causing a wide range of infections, although some lineages have also been described as plant endophytes [49]. Indeed, several *Enterobacter* species can colonize internal plant tissues, improve plant growth and prevent from pathogens attacks [70–74]. Thus, *Enterobacter cloacae* was found to halt fungal phytopathogens growth such as *Phytophthora blight* by 35.13% and *Rhizoctonia solani* with pathogen growth inhibition up to 60% [75]. Additionally, *E. cloacae* inhibited the development of *Pythium myriotyrum*, *Gaeumannomyces graminis* and *Heterobasidion annosum* [52].

The observed inhibition is due to production of several antifungal metabolites such as H₂S, ammonia and volatile compounds such as phenylethyl alcohol, 4,5-dimethyl-1-hexene, and butyl acetate that halt the growth of fungal phytopathogens [50,76]. Recently, it has been reported that *E. cloacae* is able to produce inorganic volatile substances such as ammonia, IAA and hydroxamate siderophore, hydrogen cyanide and salicylic acid [74,77], in addition to chitinase, cellulase, and beta-glucosidase enzyme all of which may participate to the biocontrol activity [73,78–80]. Furthermore, Chaouachi et al. [81] reported for the first time volatile organic compounds (VOCs) with antifungal activity produced by *E. cloacae* against *B. cinerea* decay on tomato fruit. Similarly, *Bacillus* species such as *B. velezensis* [63,82] are known to produce antifungal VOCs against several phytopathogens including *B. cinerea*.

In addition, Patel et al. [83] and Agbodjato et al. [84] reported that AIA with ammonia production prevents the development of various plant pathogenic fungi and enhance the plant growth. Additionally, solubilization of phosphate and potassium occurs due to the production of protons and oxalic, tartaric acid and polysaccharidic capsules by bacteria [76,85]. Romero et al. [86] have reported that antimicrobial compounds produced by

Bacillus spp. are mainly classified into two categories: ribosome-synthesized peptides such as bacteriocin, and small microbial peptides enzymatically synthesized by non-ribosomal pathways, mainly cyclic lipopeptides (CLPs). Since *B. velezensis* is not pathogenic to humans, different strains of *B. velezensis*, which is a typical PGPR, have received significant attention in the last decade.

So far, *B. velezensis* was described to halt the growth of many pathogenic fungi, such as *Aspergillus flavus* [87], *Cylindrocladium quinqueseptatum*, *Cryphonectria parasitica* and *Helicobasidium purpureum* [88], *Fusarium oxysporum* and *Ralstonia solanacearum* [89], and *Rhizoctonia solani* AG1-IB [90], by the biosynthesis of β -1,3-1,4-glucanase, lipopeptide antibiotics (surfactin, iturin, and fengycin, for example), polyketides (actinomycin D, bacitracin, and cyclosporin A, for example), siderophores, and NH₃ [44,91–93]. These data are in line with our in silico analysis of both bacteria *B. velezensis* S3 and *E. cloacae* S6. Thus, analysis of *E. cloacae* S6 genome pointed out the presence of non-ribosomal peptide synthetase (NRPS) and bacteriocin, while the genome of strain *B. velezensis* S3 revealed different SMGCs, such as bacillibactin, fengycin, surfactin and bacillaene. Hence, it was hypothesized that these strains might produce a variety of antifungal compounds that participate in the control of the grapevine GM disease.

The photosynthesis provides near 90–95% of plants dry matter and the metabolic energy needed for plant's development. Pathogen attack not only impact plant defenses reactions but can also lead to changes in the rate of photosynthesis and therefore the carbohydrates metabolism [37]. Hence, four days after infection, it appears that under *Botrytis* exposure, thermal dissipation in control was down-regulated not due to an increased PSII quantum efficiency, but due to an increased nonregulated energy loss in PSII, suggesting that both photochemical energy conversion and protective regulatory mechanism were insufficient [94]. Consequently, the larger portion of absorbed light energy is allocated to nonregulated energy loss in PSII [95]. The latter parameter indicates an irreversible damage of photosynthetic apparatus as confirmed by the decreased Fv/Fm ratio, since the Y(NO) leads to the formation of singlet oxygen via the triplet state of chlorophyll (3chl*) [96,97]. In line with our results, several reports on photosynthesis have indicated that photosynthesis rates are altered after infection with several plant pathogens [4,95]. We also have observed that the regulation of mechanisms involved in nonphotochemical dissipation of energy was blocked, making grapevine plantlets unable to protect themselves against damage from excess illumination [37]. A significant decline of effective quantum yield of PSII(Y(II)) complemented by a quantum yield of regulated energy dissipation nonphotochemical chlorophyll fluorescence quenching [Y(NPQ)] increase was observed after the *B. cinerea* infection. The [Y(NPQ)] is a molecular adaptation that represents the fastest response of the photosynthetic membrane to excess light. It is a protective process in which excess absorbed light energy is dissipated into heat [98,99] and prevent the photosynthetic apparatus from oxidative damage [100]. However, the irreversible damages described above were prevented/attenuated when grapevine plantlets were bacterized either with *B. velezensis* S3 and *E. cloacae* S6, probably by restricting mycelial development, and therefore protecting photosynthesis apparatus. Therefore, finding safe and eco-friendly alternatives to synthetic fungicides is urgently needed to control postharvest diseases of fruit [101]. Hence, this study provided new biotechnologies by reporting for the first time that following root inoculation, *B. velezensis* S3 and *E. cloacae* S6 allowing grapevine to better resist aerial parasitic pressures of *B. cinerea* while at the same time prevent grapevine from considerable photo-inhibition.

5. Conclusions

In conclusion, both bacteria screened as efficient anti-*Botrytis* were identified as *B. velezensis* S3 and *E. cloacae* S6. In silico analysis of draft genome sequences of *B. velezensis* S3 indicates the presence of gene clusters involved in amino acids and derivatives synthesis, carbohydrates and proteins metabolism, cofactors, vitamins, prosthetic groups and pigment formations, and stress response; while that of the *E. cloacae* S6 revealed the presence of

different secondary metabolites gene clusters, including bacillibactin, fengycin, surfactin and bacillaene and the presence of non-ribosomal peptide synthetase and bacteriocin.

Further work is obviously required to characterize how these bacteria trigger the biotic stress resistance in plants to establish a set of biotic stress biomarkers that might help to predict efficacy of induced resistance for different crops. In addition, it would also be very interesting to analyze the plant's response to colonization, i.e., lipid content, fatty acid composition as well as secondary metabolites profiles.

Nevertheless, genus *Enterobacter* is a member of the ESKAPE group, which contains the major opportunistic and multi-resistant bacterial pathogens for humans during recent decades in hospital wards. Therefore, a deeper progress in genome sequencing of *E. cloacae* S6 is critical before a potential use of this strain for plant protection. Additionally, deciphering the mechanisms of horizontal gene transfer that may occur in specific microhabitats may be a key step in the development of a regulatory framework for the environmental release of these bacteria.

Supplementary Materials: Supplementary materials can be found at <https://www.mdpi.com/article/10.3390/microorganisms9071386/s1>. Table S1. Project information of the draft genome sequences of the strains. Figure S1. Proportion of different structure in a fatty acid profile of isolated strains. Figure S2. Subsystem information of the strain *B. velezensis* S3 and *E. cloacae* S6 and predicted by SEED viewer, most of which were involved in amino acids and derivatives synthesis, carbohydrate metabolism, cofactors, vitamins, prosthetic groups and pigment formations, and stress response.

Author Contributions: Conceptualization, E.A.B., N.V.-G. and M.H.; methodology, E.A.B., N.V.-G., M.H., L.S. and Q.E.; software, Q.E.; validation, E.A.B., N.V.-G., and M.H.; formal analysis, E.A.B., N.V.-G., L.S., Z.A., and Q.E.; investigation, E.A.B., Q.E., N.V.-G., and M.H.; resources, E.A.B., Q.E., N.V.-G. and M.H.; data curation, E.A.B., N.V.-G., Z.A., and M.H.; writing—original draft preparation, E.A.B., Q.E., N.V.-G., M.H. and Z.A.; writing—review and editing, E.A.B., Q.E., N.V.-G., Z.A., and M.H.; supervision, E.A.B., N.V.-G., C.J., and M.H.; project administration, E.A.B., N.V.-G. and M.H.; funding acquisition, E.A.B., N.V.-G. and M.H. All authors have read and agreed to the published version of the manuscript.

Funding: This work was supported by the University of Reims Champagne-Ardenne, and the University Moulay Ismail-Faculty of Sciences via the attribution of the doctoral grant.

Conflicts of Interest: The authors declare no conflict of interest.

References

1. Rojas, C.M.; Senthil-Kumar, M.; Tzin, V.; Mysore, K.S. Regulation of primary plant metabolism during plant-pathogen interactions and its contribution to plant defense. *Front. Plant Sci.* **2014**, *5*, 17. [CrossRef]
2. Verdenal, T.; Dienes-Nagy, Á.; Spangenberg, J.E.; Zufferey, V.; Spring, J.; Viret, O.; Marin-Carbonne, J.; van Leeuwen, C. Understanding and managing nitrogen nutrition in grapevine: A review. *OENO One* **2021**, *55*, 1–43. [CrossRef]
3. Júnior, A.F.N.; Tränkner, M.; Ribeiro, R.V.; von Tiedemann, A.; Amorim, L. Photosynthetic Cost Associated With Induced Defense to *Plasmopara viticola* in Grapevine. *Front. Plant Sci.* **2020**, *11*, 1–14. [CrossRef]
4. Bonfig, K.B.; Schreiber, U.; Gabler, A.; Roitsch, T.; Berger, S. Infection with virulent and avirulent *P. syringae* strains differentially affects photosynthesis and sink metabolism in Arabidopsis leaves. *Planta* **2006**, *225*, 1–12. [CrossRef] [PubMed]
5. Nascimento, R.; Maia, M.; Ferreira, A.E.N.; Silva, A.B.; Freire, A.P.; Cordeiro, C.; Silva, M.S.; Figueiredo, A. Early stage metabolic events associated with the establishment of *Vitis vinifera*–*Plasmopara viticola* compatible interaction. *Plant Physiol. Biochem.* **2019**, *137*, 1–13. [CrossRef]
6. Jones, D.J.L.; Dangl, J.L. The plant immune system. *Nature* **2006**, *444*, 323–329. [CrossRef] [PubMed]
7. Windram, O.; Denby, K.J. Modelling signaling networks underlying plant defence. *Curr. Opin. Plant Biol.* **2015**, *27*, 165–171. [CrossRef] [PubMed]
8. De Lorenzo, G.; Ferrari, S.; Cervone, F.; Okun, E. Extracellular DAMPs in Plants and Mammals: Immunity, Tissue Damage and Repair. *Trends Immunol.* **2018**, *39*, 937–950. [CrossRef]
9. Fillinger, S.; Yigal, E. *Botrytis—The Fungus, the Pathogen and Its Management in Agricultural Systems*; Springer: Berlin/Heidelberg, Germany, 2016.
10. Dean, R.; Van-Kan, J.A.; Pretorius, Z.A.; Hammond-Kosack, K.E.; Di-Pietro, A.; Spanu, P.D.; Rudd, J.J.; Dickman, M.; Kahmann, R.; Ellis, J.; et al. The Top 10 fungal pathogens in molecular plant pathology. *Mol. Plant Pathol.* **2012**, *13*, 414–430. [CrossRef]
11. Weiberg, A.; Wang, M.; Lin, F.-M.; Zhao, H.; Zhang, Z.; Kaloshian, I.; Huang, H.; Jin, H. Fungal Small RNAs Suppress Plant Immunity by Hijacking Host RNA Interference Pathways. *Science* **2013**, *342*, 118–123. [CrossRef]

12. Boddy, L. *Pathogens of Autotrophs*, 3rd ed.; Watkinson, S.C., Boddy, L., Money, N.P., Eds.; Academic Press: Boston, MA, USA, 2016; pp. 245–292, Chapter 8.
13. Fernández-Ortuño, D.; Torés, J.A.; Chamorro, M.; Pérez-García, A.; de Vicente, A. Characterization of resistance to six chemical classes of site-specific fungicides registered for gray mold control on strawberry in Spain. *Plant Dis.* **2016**, *100*, 2234–2239. [[CrossRef](#)]
14. Rupp, S.; Weber, R.W.S.; Rieger, D.; Detzel, P.; Hahn, M. Spread of *Botrytis cinerea* strains with multiple fungicide resistance in german horticulture. *Front. Microbiol.* **2017**, *7*. [[CrossRef](#)] [[PubMed](#)]
15. Yin, W.X.; Adnan, M.; Shang, Y.; Lin, Y.; Luo, C.X. Sensitivity of *Botrytis cinerea* from nectarine/cherry in China to six fungicides and characterization of resistant isolates. *Plant Dis.* **2018**, *102*, 2578–2585. [[CrossRef](#)] [[PubMed](#)]
16. Sautua, F.J.; Baron, C.; Pérez-Hernández, O.; Carmona, M.A. First report of resistance to carbendazim and procymidone in *Botrytis cinerea* from strawberry, blueberry and tomato in Argentina. *Crop Prot.* **2019**, *125*, 2017–2020. [[CrossRef](#)]
17. Reeves, W.R.; McGuire, M.K.; Stokes, M.; Vicini, J.L. Assessing the Safety of Pesticides in Food: How Current Regulations Protect Human Health. *Adv. Nutr.* **2019**, *10*, 80–88. [[CrossRef](#)]
18. Liu, J.; Sui, Y.; Wisniewski, M.; Droby, S.; Liu, Y. Review: Utilization of antagonistic yeasts to manage postharvest fungal diseases of fruit. *Int. J. Food Microbiol.* **2013**, *167*, 153–160. [[CrossRef](#)]
19. Liu, Y.; Wang, W.; Zhou, Y.; Yao, S.; Deng, L.; Zeng, K. Isolation, identification and in vitro screening of Chongqing orangery yeasts for the biocontrol of *Penicillium digitatum* on citrus fruit. *Biol. Control* **2017**, *110*, 18–24. [[CrossRef](#)]
20. Romanazzi, G.; Feliziani, E.; Bautista-Baños, S.; Sivakumar, D. Shelf Life Extension of Fresh Fruit and Vegetables by Chitosan Treatment. *Crit. Rev. Food Sci. Nutr.* **2017**, *57*. [[CrossRef](#)]
21. Li, T.; Li, H.; Liu, T.; Zhu, J.; Zhang, L.; Mu, W.; Liu, F. Evaluation of the antifungal and biochemical activities of mefentrifluconazole against *Botrytis cinerea*. *Pestic. Biochem. Physiol.* **2021**, 104784. [[CrossRef](#)]
22. Pertot, I.; Caffi, T.; Rossi, V.; Mugnai, L.; Hoffmann, C.; Grando, M.S.; Gary, C.; Lafond, D.; Duso, C.; Thiery, D.; et al. A critical review of plant protection tools for reducing pesticide use on grapevine and new perspectives for the implementation of IPM in viticulture. *Crop Prot.* **2017**, *97*, 70–84. [[CrossRef](#)]
23. Deshwal, V.K.; Pandey, P.; Kang, S.C.; Maheshwari, D.K. Rhizobia as a biological control agent against soil borne plant pathogenic fungi. *Indian J. Exp. Biol.* **2003**, *41*, 1160–1164. [[PubMed](#)]
24. Lugtenberg, B.; Kamilova, F. Plant-Growth-Promoting Rhizobacteria. *Annu. Rev. Microbiol.* **2009**, *63*, 541–556. [[CrossRef](#)]
25. Kumar, H.; Bajpai, V.K.; Dubey, R.C.; Maheshwari, D.K.; Kang, S.C. Wilt disease management and enhancement of growth and yield of *Cajanus cajan* (L) var. Manak by bacterial combinations amended with chemical fertilizer. *Crop Prot.* **2010**, *29*, 591–598. [[CrossRef](#)]
26. Peian, Z.; Haifeng, J.; Peijie, G.; Sadeghnezhad, E.; Qianqian, P.; Tianyu, D.; Teng, L.; Huanchun, J.; Jinggui, F. Chitosan induces jasmonic acid production leading to resistance of ripened fruit against *Botrytis cinerea* infection. *Food Chem.* **2021**, *337*, 127772. [[CrossRef](#)] [[PubMed](#)]
27. Platania, C.; Restuccia, C.; Muccilli, S.; Cirvilleri, G. Efficacy of killer yeasts in the biological control of *Penicillium digitatum* on Tarocco orange fruits (*Citrus sinensis*). *Food Microbiol.* **2012**, *30*, 219–225. [[CrossRef](#)] [[PubMed](#)]
28. Yang, J.; Klopper, J.W.; Ryu, C.M. Rhizosphere bacteria help plants tolerate abiotic stress. *Trends Plant Sci.* **2009**, *14*, 1–4. [[CrossRef](#)]
29. Nally, M.C.; Pesce, V.M.; Maturano, Y.P.; Muñoz, C.J.; Combina, M.; Toro, M.E.; de Figueroa, L.C.; Vazquez, F. Biocontrol of *Botrytis cinerea* in table grapes by non-pathogenic indigenous *Saccharomyces cerevisiae* yeasts isolated from viticultural environments in Argentina. *Postharvest Biol. Technol.* **2012**, *64*, 40–48. [[CrossRef](#)]
30. Esmaeel, Q.; Jacquard, C.; Clément, C.; Sanchez, L.; Ait, E.; Barka, E.A. Genome sequencing and traits analysis of *Burkholderia* strains reveal a promising biocontrol effect against grey mould disease in grapevine (*Vitis vinifera* L.). *World J. Microbiol. Biotechnol.* **2019**, *35*. [[CrossRef](#)] [[PubMed](#)]
31. Thompson, J.D.; Gibson, T.J.; Plewniak, F.; Jeanmougin, F.; Higgins, D.G. The CLUSTAL X windows interface: Flexible strategies for multiple sequence alignment aided by quality analysis tools. *Nucleic Acids Res.* **1997**, *25*, 4876–4882. [[CrossRef](#)]
32. Tamura, K.; Peterson, D.; Peterson, N.; Stecher, G.; Nei, M.; Kumar, S. MEGA5: Molecular evolutionary genetics analysis using maximum likelihood, evolutionary distance, and maximum parsimony methods. *Mol. Biol. Evol.* **2011**, *28*, 2731–2739. [[CrossRef](#)]
33. Aziz, R.K.; Bartels, D.; Best, A.A.; DeJongh, M.; Disz, T.; Edwards, R.A.; Formsma, K.; Gerdes, S.; Glass, E.M.; Kubal, M.; et al. The RAST Server: Rapid annotations using subsystems technology. *BMC Genom.* **2008**, *9*, 363. [[CrossRef](#)] [[PubMed](#)]
34. Disz, T.; Akhter, S.; Cuevas, D.; Olson, R.; Overbeek, R.; Vonstein, V.; Stevens, R.; Edwards, R.A. Accessing the SEED Genome Databases via Web Services API: Tools for Programmers. *BMC Bioinform.* **2010**, *11*, 319. [[CrossRef](#)]
35. Weber, T.; Blin, K.; Duddela, S.; Krug, D.; Kim, H.U.; Brucoleri, R.; Lee, S.Y.; Fischbach, M.A.; Müller, R.; Wohlleben, W.; et al. AntiSMASH 3.0-A comprehensive resource for the genome mining of biosynthetic gene clusters. *Nucleic Acids Res.* **2015**, *43*, W237–W243. [[CrossRef](#)] [[PubMed](#)]
36. Barka, E.A.; Nowak, J.; Clément, C. Enhancement of chilling resistance of inoculated grapevine plantlets with a plant growth-promoting rhizobacterium, *Burkholderia phytofirmans* strain PsJN. *Appl. Environ. Microbiol.* **2006**, *72*, 7246–7252. [[CrossRef](#)]
37. Miotto-Vilanova, L.; Jacquard, C.; Courteaux, B.; Wortham, L.; Michel, J.; Clément, C.; Barka, E.A.; Sanchez, L. *Burkholderia phytofirmans* PsJN Confers Grapevine Resistance against *Botrytis cinerea* via a Direct Antimicrobial Effect Combined with a Better Resource Mobilization. *Front. Plant Sci.* **2016**, *7*, 1236. [[CrossRef](#)] [[PubMed](#)]

38. Genty, B.; Briantais, J.-M.; Baker, N.R. The relationship between the quantum yield of photosynthetic electron transport and quenching of chlorophyll fluorescence. *Biochim. Biophys. Acta Gen. Subj.* **1989**, *990*, 87–92. [CrossRef]
39. Kramer, D.M.; Johnson, G.; Kiirats, O.; Edwards, G.E. New fluorescence parameters for the determination of QA redox state and excitation energy fluxes. *Photosynth. Res.* **2004**, *79*, 209–218. [CrossRef] [PubMed]
40. Rodríguez-R, L.M.; Gunturu, S.; Harvey, W.T.; Rosselló-Mora, R.; Tiedje, J.M.; Cole, J.R.; Konstantinidis, K.T. The Microbial Genomes Atlas (MiGA) webserver: Taxonomic and gene diversity analysis of Archaea and Bacteria at the whole genome level. *Nucleic Acids Res.* **2018**, *46*, W282–W288. [CrossRef]
41. Meier-Kolthoff, J.P.; Göker, M. TYGS is an automated high-throughput platform for state-of-the-art genome-based taxonomy. *Nat. Commun.* **2019**, *10*, 2182. [CrossRef]
42. Sasse, J.; Martinoia, E.; Northen, T. Feed Your Friends: Do Plant Exudates Shape the Root Microbiome? *Trends Plant Sci.* **2018**, *23*, 25–41. [CrossRef] [PubMed]
43. Wang, C.; Zhao, D.; Qi, G.; Mao, Z.; Hu, X.; Du, B.; Liu, K.; Ding, Y. Effects of *Bacillus velezensis* FKM10 for Promoting the Growth of *Malus hupehensis* Rehd. and Inhibiting *Fusarium verticillioides*. *Front. Microbiol.* **2020**, *10*, 2889. [CrossRef] [PubMed]
44. Meng, Q.; Jiang, H.; Hao, J.J. Effects of *Bacillus velezensis* strain BAC03 in promoting plant growth. *Biol. Control* **2016**, *98*, 18–26. [CrossRef]
45. Taghavi, S.; van der Lelie, D.; Hoffman, A.; Zhang, Y.; Walla, M.D.; Vangronsveld, J.; Newman, L.; Monchy, S. Genome sequence of the plant growth promoting endophytic bacterium *Enterobacter* sp. 638. *PLoS Genet.* **2010**, *6*, 19. [CrossRef] [PubMed]
46. Macedo-Raygoza, G.M.; Valdez-Salas, B.; Prado, F.M.; Prieto, K.R.; Yamaguchi, L.F.; Kato, M.J.; Canto-Canché, B.B.; Carrillo-Beltrán, M.; di Mascio, P.; White, J.F.; et al. *Enterobacter cloacae*, an endophyte that establishes a nutrient-transfer symbiosis with banana plants and protects against the black sigatoka pathogen. *Front. Microbiol.* **2019**, *10*, 804. [CrossRef] [PubMed]
47. Toral, L.; Rodríguez, M.; Béjar, V.; Sampedro, I. microorganisms Crop Protection against *Botrytis cinerea* by Rhizosphere Biological Control Agent *Bacillus velezensis* XT1. *Microorganisms* **2020**, *8*, 992. [CrossRef]
48. Chen, L.; Wang, X.; Ma, Q.; Bian, L.; Liu, X.; Xu, Y.; Zhang, H.; Shao, J.; Liu, Y. *Bacillus velezensis* CLA178-Induced Systemic Resistance of *Rosa multiflora* Against Crown Gall Disease. *Front. Microbiol.* **2020**, *11*, 587667. [CrossRef] [PubMed]
49. Shastry, R.P.; Welch, M.; Rai, V.R.; Ghate, S.D.; Sandeep, K.; Rekha, P.D. The whole-genome sequence analysis of *Enterobacter cloacae* strain Ghats1: Insights into endophytic lifestyle-associated genomic adaptations. *Arch. Microbiol.* **2020**, *202*, 1571–1579. [CrossRef]
50. Shi, J.F.; Sun, C.Q. Isolation, identification, and biocontrol of antagonistic bacterium against *Botrytis cinerea* after tomato harvest. *Braz. J. Microbiol.* **2017**, *48*, 706–714. [CrossRef] [PubMed]
51. Pan, H.Q.; Li, Q.L.; Hu, J.C. The complete genome sequence of *Bacillus velezensis* 9912D reveals its biocontrol mechanism as a novel commercial biological fungicide agent. *J. Biotechnol.* **2017**, *247*, 25–28. [CrossRef]
52. Wang, F.; Xiao, J.; Zhang, Y.; Li, R.; Liu, L.; Deng, J. Biocontrol ability and action mechanism of *Bacillus halotolerans* against *Botrytis cinerea* causing grey mould in postharvest strawberry fruit. *Postharvest Biol. Technol.* **2021**, *174*, 111456. [CrossRef]
53. Gordon, R.E.; Haynes, W.C.; Pang, C.H.-N.; Smith, N.R. *The Genus Bacillus*; Agricultural Research Service, U.S. Department of Agriculture: Washington, DC, USA, 1973. Available online: <http://books.google.com/books?id=IXMpXssWFD0C> (accessed on 3 June 2021).
54. Priest, F.G.; Goodfellow, M. *Bacillus amyloliquefaciens* sp. nov. norn. rev. *Microbiol. Soc.* **1987**. [CrossRef]
55. Ruiz-García, C.; Béjar, V.; Martínez-Checa, F.; Llamas, I.; Quesada, E. *Bacillus velezensis* sp. nov., a surfactant-producing bacterium isolated from the river Vélez in Málaga, southern Spain. *Int. J. Syst. Evol. Microbiol.* **2005**, *55*, 191–195. [CrossRef]
56. Madhaiyan, M.; Poonguzhali, S.; Kwon, S.W.; Sa, T.M. *Bacillus methylotrophicus* sp. nov., a methanol-utilizing, plant-growth-promoting bacterium isolated from rice rhizosphere soil. *Int. J. Syst. Evol. Microbiol.* **2010**, *60*, 2490–2495. [CrossRef] [PubMed]
57. Dunlap, C.A.; Bowman, M.J.; Schisler, D.A.; Rooney, A.P. Genome analysis shows *Bacillus axarquiensis* is not a later heterotypic synonym of *Bacillus mojavensis*; reclassification of *Bacillus malacitensis* and *Brevibacterium halotolerans* as heterotypic synonyms of *Bacillus axarquiensis*. *Int. J. Syst. Evol. Microbiol.* **2016**, *66*, 2438–2443. [CrossRef] [PubMed]
58. Dunlap, C.A.; Kim, S.J.; Kwon, S.W.; Rooney, A.P. *Bacillus velezensis* is not a later heterotypic synonym of *Bacillus amyloliquefaciens*; *Bacillus methylotrophicus*, *Bacillus amyloliquefaciens* subsp. *Plantarum* and '*Bacillus oryzicola*' are later heterotypic synonyms of *Bacillus velezensis* based on phylogenom. *Int. J. Syst. Evol. Microbiol.* **2016**, *66*, 1212–1217. [CrossRef]
59. Dunlap, C.A.; Kim, S.-J.; Kwon, S.-W.; Rooney, A.P. Phylogenomic analysis shows that *Bacillus amyloliquefaciens* subsp. *plantarum* is a later heterotypic synonym of *Bacillus methylotrophicus*. *Int. J. Syst. Evol. Microbiol.* **2015**, *65*, 2104–2109. [CrossRef] [PubMed]
60. Wu, L.; Wu, H.J.; Qiao, J.; Gao, X.; Borriss, R. Novel routes for improving biocontrol activity of *Bacillus* based bioinoculants. *Front. Microbiol.* **2015**, *6*, 1395. [CrossRef]
61. Fan, B.; Blom, J.; Klenk, H.P.; Borriss, R. *Bacillus amyloliquefaciens*, *Bacillus velezensis*, and *Bacillus siamensis* Form an 'Operational Group *B. amyloliquefaciens*' within the *B. subtilis* species complex. *Front. Microbiol.* **2017**, *8*, 22. [CrossRef]
62. Myo, E.M.; Liu, B.; Ma, J.; Shi, L.; Jiang, M.; Zhang, K.; Ge, B. Evaluation of *Bacillus velezensis* NKG-2 for bio-control activities against fungal diseases and potential plant growth promotion. *Biol. Control* **2019**, *134*, 23–31. [CrossRef]
63. Jiang, C.H.; Liao, M.J.; Wang, H.K.; Zheng, M.Z.; Xu, J.J.; Guo, J.H. *Bacillus velezensis*, a potential and efficient biocontrol agent in control of pepper gray mold caused by *Botrytis cinerea*. *Biol. Control* **2018**, *126*, 147–157. [CrossRef]
64. Gao, Z.; Zhang, B.; Liu, H.; Han, J.; Zhang, Y. Identification of endophytic *Bacillus velezensis* ZSY-1 strain and antifungal activity of its volatile compounds against *Alternaria solani* and *Botrytis cinerea*. *Biol. Control* **2017**, *105*, 27–39. [CrossRef]

65. Xu, Z.; Zhang, H.; Sun, X.; Liu, Y.; Yan, W.; Xun, W.; Shen, Q.; Zhang, R. *Bacillus velezensis* wall teichoic acids are required for biofilm. *Appl. Environ. Microbiol.* **2019**, *85*, e02116-18. [[CrossRef](#)]
66. Morales-Cedeño, L.R.; Orozco-Mosqueda, M.D.; Loeza-Lara, P.D.; Parra-Cota, F.I.; de los Santos-Villalobos, S.; Santoyo, G. Plant growth-promoting bacterial endophytes as biocontrol agents of pre- and post-harvest diseases: Fundamentals, methods of application and future perspectives. *Microbiol. Res.* **2021**, *242*, 12. [[CrossRef](#)]
67. Lima, G.; de Curtis, F.; Piedimonte, D.; Spina, A.M.; de Cicco, V. Integration of biocontrol yeast and thiabendazole protects stored apples from fungicide sensitive and resistant isolates of *Botrytis cinerea*. *Postharvest Biol. Technol.* **2006**, *40*, 301–307. [[CrossRef](#)]
68. Püttmann, M.; Ade, N.; Hof, H. Dependence of fatty acid composition of *Listeria* spp. on growth temperature. *Res. Microbiol.* **1993**, *144*, 279–283. [[CrossRef](#)]
69. Annous, B.A.; Becker, L.A.; Bayles, D.O.; Labeda, D.P.; Wilkinson, B.J. Critical role of anteiso-C(15:0) fatty acid in the growth of *Listeria monocytogenes* at low temperatures. *Appl. Environ. Microbiol.* **1997**, *63*, 3887–3894. [[CrossRef](#)]
70. Fernández-González, A.J.; Martínez-Hidalgo, P.; Cobo-Díaz, J.F.; Villadas, P.J.; Martínez-Molina, E.; Toro, N.; Tringe, S.G.; Fernández-López, M. The rhizosphere microbiome of burned holm-oak: Potential role of the genus *Arthrobacter* in the recovery of burned soils. *Sci. Rep.* **2017**, *7*, 1–12. [[CrossRef](#)] [[PubMed](#)]
71. Tsuda, K.; Kosaka, Y.; Tsuge, S.; Kubo, Y.; Horino, O. Evaluation of the Endophyte *Enterobacter cloacae* SM10 Isolated from Spinach Roots for Biological Control against Fusarium Wilt of Spinach. *J. Gen. Plant Pathol.* **2001**, *67*, 78–84. [[CrossRef](#)]
72. Latha, P.; Karthikeyan, M.; Rajeswari, E. *Plant Health under Biotic Stress*; Springer: Berlin/Heidelberg, Germany, 2019.
73. Guo, D.J.; Singh, R.K.; Singh, P.; Li, D.P.; Sharma, A.; Xing, Y.X.; Song, X.P.; Yang, L.T.; Li, Y.R. Complete Genome Sequence of *Enterobacter roggenskampi* ED5, a Nitrogen Fixing Plant Growth Promoting Endophytic Bacterium with Biocontrol and Stress Tolerance Properties, Isolated From Sugarcane Root. *Front. Microbiol.* **2020**, *11*, 28. [[CrossRef](#)]
74. Mohamed, B.F.F.; Sallam, N.M.A.; Alamri, S.A.M.; Abo-Elyousr, K.A.M.; Mostafa, Y.S.; Hashem, M. Approving the biocontrol method of potato wilt caused by *Ralstonia solanacearum* (Smith) using *Enterobacter cloacae* PS14 and *Trichoderma asperellum* T34. *Egypt. J. Biol. Pest Control* **2020**, *30*, 13. [[CrossRef](#)]
75. Abdeljalil, N.O.; Vallance, J.; Gerbore, J.; Yacoub, A.; Daami-Remadi, M.; Rey, P. Combining potential oomycete and bacterial biocontrol agents as a tool to fight tomato Rhizoctonia root rot. *Biol. Control* **2021**, *155*, 104521. [[CrossRef](#)]
76. Chen, P.-S.; Peng, Y.-H. Inhibition of *Penicillium digitatum* and Citrus Green Mold by Volatile Compounds Produced by *Enterobacter cloacae*. *J. Plant Pathol. Microbiol.* **2016**, *7*. [[CrossRef](#)]
77. Singh, R.P.; Nalwaya, S.; Jha, P.N. The draft genome sequence of the plant growth promoting rhizospheric bacterium *Enterobacter cloacae* SBP-8. *Genom. Data* **2017**, *12*, 81–83. [[CrossRef](#)]
78. Cho, S.T.; Chang, H.H.; Egamberdieva, D.; Kamilova, F.; Lugtenberg, B.; Kuo, C.H. Genome analysis of *Pseudomonas fluorescens* PCL1751: A rhizobacterium that controls root diseases and alleviates salt stress for its plant host. *PLoS ONE* **2015**, *10*, e0140231. [[CrossRef](#)]
79. Luo, Y.; Cheng, Y.; Yi, J.; Zhang, Z.; Luo, Q.; Zhang, D.; Li, Y. Complete genome sequence of industrial biocontrol strain *Paenibacillus polymyxa* HY96-2 and further analysis of its biocontrol mechanism. *Front. Microbiol.* **2018**, *9*, 1520. [[CrossRef](#)] [[PubMed](#)]
80. Yang, E.; Sun, L.; Ding, X.; Sun, D.; Liu, J.; Wang, W. Complete genome sequence of *Caulobacter flavus* RHGG3T, a type species of the genus *Caulobacter* with plant growth-promoting traits and heavy metal resistance. *3 Biotech* **2019**, *9*, 42. [[CrossRef](#)] [[PubMed](#)]
81. Chaouachi, M.; Marzouk, T.; Jallouli, S.; Elkahoui, S.; Gentzbittel, L.; Ben, C.; Djébali, N. Activity assessment of tomato endophytic bacteria bioactive compounds for the postharvest biocontrol of *Botrytis cinerea*. *Postharvest Biol. Technol.* **2021**, *172*, 18. [[CrossRef](#)]
82. Gao, H.; Li, P.; Xu, X.; Zeng, Q.; Guan, W. Research on volatile organic compounds from *Bacillus subtilis* CF-3: Biocontrol effects on fruit fungal pathogens and dynamic changes during fermentation. *Front. Microbiol.* **2018**, *9*. [[CrossRef](#)]
83. Patel, P.; Shah, R.; Modi, K. Isolation and characterization of plant growth promoting potential of *Acinetobacter* sp. RSC7 isolated from *Saccharum officinarum* cultivar Co 671. *J. Exp. Biol. Agric. Sci.* **2017**, *5*, 483–491. [[CrossRef](#)]
84. Agbodjato, N.A.; Noumavo, P.A.; Baba-Moussa, F.; Salami, H.A.; Sèzan, A.; Bankolé, H.; Adjanohoun, A.; Baba-Moussa, L. Characterization of potential plant growth promoting rhizobacteria isolated from Maize (*Zea mays* L.) in central and Northern Benin (West Africa). *Appl. Environ. Soil Sci.* **2015**, *2015*. [[CrossRef](#)]
85. Bashan, Y.; Kamnev, A.A.; de-Bashan, L.E. Tricalcium phosphate is inappropriate as a universal selection factor for isolating and testing phosphate-solubilizing bacteria that enhance plant growth: A proposal for an alternative procedure. *Biol. Fertil. Soils* **2013**, *49*, 465–479. [[CrossRef](#)]
86. Romero, D.; de Vicente, A.; Rakotoaly, R.H.; Dufour, S.E.; Veening, J.W.; Arrebola, E.; Cazorla, F.M.; Kuipers, O.P.; Paquot, M.; Pérez-García, A. The iturin and fengycin families of lipopeptides are key factors in antagonism of *Bacillus subtilis* toward *Podosphaera fusca*. *Mol. Plant Microbe Interact.* **2007**, *20*, 430–440. [[CrossRef](#)] [[PubMed](#)]
87. Chen, L.; Shi, H.; Heng, J.; Wang, D.; Bian, K. Antimicrobial, plant growth-promoting and genomic properties of the peanut endophyte *Bacillus velezensis* LDO2. *Microbiol. Res.* **2019**, *218*, 41–48. [[CrossRef](#)]
88. Xu, T.; Zhu, T.; Li, S. β -1,3,1,4-glucanase gene from *Bacillus velezensis* ZJ20 exerts antifungal effect on plant pathogenic fungi. *World J. Microbiol. Biotechnol.* **2016**, *32*, 26. [[CrossRef](#)]
89. Cao, Y.; Pi, H.; Chandransu, P.; Li, Y.; Wang, Y.; Zhou, H.; Xiong, H.; Helmann, J.D.; Cai, Y. Antagonism of Two Plant-Growth Promoting *Bacillus velezensis* Isolates Against *Ralstonia solanacearum* and *Fusarium oxysporum*. *Sci. Rep.* **2018**, *8*, 4360. [[CrossRef](#)] [[PubMed](#)]

90. Chowdhury, S.P.; Dietel, K.; Rändler, M.; Schmid, M.; Junge, H.; Borriss, R.; Hartmann, A.; Grosch, R. Effects of *Bacillus amyloliquefaciens* FZB42 on Lettuce Growth and Health under Pathogen Pressure and Its Impact on the Rhizosphere Bacterial Community. *PLoS ONE* **2013**, *8*, e68818. [[CrossRef](#)]
91. Kim, S.Y.; Song, H.; Sang, M.K.; Weon, H.Y.; Song, J. The complete genome sequence of *Bacillus velezensis* strain GH1-13 reveals agriculturally beneficial properties and a unique plasmid. *J. Biotechnol.* **2017**, *259*, 221–227. [[CrossRef](#)]
92. Adeniji, A.A.; Loots, D.T.; Babalola, O.O. *Bacillus velezensis*: Phylogeny, useful applications, and avenues for exploitation. *Appl. Microbiol. Biotechnol.* **2019**, *103*, 3669–3682. [[CrossRef](#)]
93. Fan, B.; Wang, C.; Song, X.; Ding, X.; Wu, L.; Wu, H.; Gao, X.; Borriss, R. *Bacillus velezensis* FZB42 in 2018: The Gram-Positive Model Strain for Plant Growth Promotion and Biocontrol. *Front. Microbiol.* **2018**, *9*, 2491. [[CrossRef](#)]
94. Calatayud, A.; Roca, D.; Martínez, P.F. Spatial-temporal variations in rose leaves under water stress conditions studied by chlorophyll fluorescence imaging. *Plant Physiol. Biochem.* **2006**, *44*, 564–573. [[CrossRef](#)]
95. Sperdoui, I.; Moustakas, M. A better energy allocation of absorbed light in photosystem II and less photooxidative damage contribute to acclimation of *Arabidopsis thaliana* young leaves to water deficit. *J. Plant Physiol.* **2014**, *171*, 587–593. [[CrossRef](#)] [[PubMed](#)]
96. Gawroński, P.; Witoń, D.; Vashutina, K.; Bederska, M.; Betliński, B.; Rusaczonek, A.; Karpiński, S. Mitogen-activated protein kinase 4 is a salicylic acid-independent regulator of growth but not of photosynthesis in *Arabidopsis*. *Mol. Plant* **2014**, *7*, 1151–1166. [[CrossRef](#)]
97. Moustaka, J.; Ouzounidou, G.; Sperdoui, I.; Moustakas, M. Photosystem II Is More Sensitive than Photosystem I to Al³⁺ Induced Phytotoxicity. *Materials* **2018**, *11*, 1772. [[CrossRef](#)]
98. Berger, S.; Sinha, A.K.; Roitsch, T. Plant physiology meets phytopathology: Plant primary metabolism and plant-pathogen interactions. *J. Exp. Bot.* **2007**, *58*, 4019–4026. [[CrossRef](#)]
99. Demmig-Adams, B.; Adams, W.W. Photoprotection in an ecological context: The remarkable complexity of thermal energy dissipation. *New Phytol.* **2006**, *172*, 11–21. [[CrossRef](#)] [[PubMed](#)]
100. Jusović, M.; Velitchkova, M.Y.; Misheva, S.P.; Börner, A.; Apostolova, E.L.; Dobrikova, A.G. Photosynthetic Responses of a Wheat Mutant (Rht-B1c) with Altered DELLA Proteins to Salt Stress. *J. Plant Growth Regul.* **2018**, *37*, 645–656. [[CrossRef](#)]
101. Guo, J.; Sun, K.; Zhang, Y.; Hu, K.; Zhao, X.; Liu, H.; Wu, S.; Hu, Y.; Zhang, Y.; Wang, Y. SIMAPK3, a key mitogen-activated protein kinase, regulates the resistance of cherry tomato fruit to *Botrytis cinerea* induced by yeast cell wall and β -glucan. *Postharvest Biol. Technol.* **2021**, *171*, 111350. [[CrossRef](#)]